KCl-Induced Phase Separation of 1,4-Dioxane + Water Mixtures Studied by Electrical Conductivity and Refractive Index†

T. Kouissi,‡ M. Bouanz,*,§ and N. Ouerfelli‡

Laboratoire de Physique des Liquides et d'Optique Non Linéaire, Département de Physique, Faculté des Sciences de Tunis, Campus Universitaire, 2092 El Manar, Tunisia, and Laboratoire de Physique des Liquides Critiques, Département de Physique, Faculté des Sciences de Bizerte, 7021 Zarzouna, Tunisia

Salt-induced phase separation of 1,4-dioxane (D) + water (W) with KCl has been investigated by measuring the electrical conductivity (κ) and the refractive index (n) along the coexisting curve in the vicinity and far from the lower critical solution temperature (LCST) using a conductometer and a refractometer. By visual method, the lower critical temperature (T_c) was determined to be (311.032 ± 0.015) K with the mole fraction of dioxane on a salt-free basis: $x'_D = n_D/(n_D + n_W) = 0.295 \pm 0.002$. The conductivity and refractive index were carried out in the range of 0.010 K < $(T - T_c)$ < 17.500 K. Critical values were fitted and compared with those predicted by models proposed in the literature. The electrical conductivity and refractive index coexistence curve data were analyzed to determine the critical exponent (β) associated with the coexistence curve. The results show that those (κ and n) constitute good order parameters as valid as the volume fraction. In the neighborhood of the LCST ($T/T_c - 1 < 3 \cdot 10^{-2}$), the critical exponent obtained by the two techniques agrees with the scaling law prediction. The KCl salt at the saturation facilitates the formation of the molecular correlations, and the phase separation takes place in the electrolyte.

Introduction

Physical and physical−chemical properties of liquid mixtures are important for understanding the thermodynamic behavior. One of the most important reasons is that these properties may provide information about intermolecular, ion−ion, and ion-molecular interactions as well as association, pair-formation, and clustering phenomena. We have been investigating and reporting data for the critical isobutyric acid + water (IBAW) mixture for many years including transport phenomena,[1] ionic structures,[2] solvation phenomena in the binary fluid,[3] the effect of ions on mixture,[4] and phase equilibrium properties occurring in the presence of added ions.[5−7] The electrical conductivity of IBAW mixtures has also been studied.[8−12] In this context, we have investigated the conductivity (κ) and the refractive index (n) along the coexisting curve of the system 1,4-dioxane + water + potassium chloride (DWKCl) and in the one-phase region near and far from the critical temperature. We note that 1,4-dioxane and water (DW) are miscible in all proportions at all temperatures. The addition of salt to a homogeneous DW mixture at a certain composition causes a phase separation, giving two conjugate phases.[14−22] Note that progressively introducing electrolytes in water + dioxane mixtures at a low dielectric constant gives evidence of the progressive association of ions pairs.[23]

Also, the study of different physicochemical properties in all of the domains of compositions shows the existence of different regions with distinct behaviors.[23] Ion−solvent and solvent−solvent interactions have been investigated.[24,25] In fact, some recent structural studies show that the dioxane and water, both proton acceptors, will cause a significant degree of H bonding, leading to strong correlation between the molecules.[26−30] When the concentration of an electrolyte increases, a phase separation in the ternary system DWKCl is often observed.

With the aim of a better understanding the critical behavior of ionic systems, we present in this Article the experimental conductivity and refractive index data along the coexistence curve of the salt-saturated DWKCl system.

This ternary system was studied under atmospheric pressure as a function of the temperature. In the one-phase region, we have also determined experimental data of the conductivity and refractive index for a fixed critical composition (on a salt-free basis) as a function of temperature. On the basis of previous remarks, we propose the order parameter for the DWKCl system. When the critical behavior of the ionic system is analyzed in terms of that choice, Ising behavior is obtained in the extend region, up to $5 \cdot 10^{-2}$ in reduced temperature. For higher distances to the critical temperature, deviations from Ising behavior are observed, and the effective exponent (β_{eff}) is presented and discussed for this system.

Experimental Procedure

Sample Preparation. The 1,4-dioxane was provided by Merck. The purity was stated to be 99.99 %. The water was obtained from deionized and three times distilled water, and it had a specific conductivity of about 10^{-6} $\Omega^{-1} \cdot cm^{-1}$ or less. The guaranteed purity of the potassium chloride (Merck product) was better than 99.5 %.

All mixtures were prepared from known masses of the pure components. The mass was obtained with a resolution of 10^{-3}g. Some care was taken to avoid moisture and dust in the final sample, namely, baking the syringes and the cells overnight under vacuum and preparing the mixtures in a dust-free area.

* To whom correspondence should be addressed. E-mail: Moncef.Bouanz@fsb.rnu.tn.
† Part of the special issue "Robin H. Stokes Festschrift".
‡ Campus Universitaire.
§ Faculté des Sciences de Bizerte.

10.1021/je8005002 CCC: $40.75
Published on Web 01/12/2009

The solution was brought to temperature equilibrium with stirring to dissolve the excess salt completely. Additional purification had not been considered to be necessary. The main impurity in the salt and 1,4-dioxane was probably water. Next, the sample was allowed to reach the equilibrium, which continued with a separation of two phases.

Electrical Conductivity Measurement. The electrical conductivity was measured with a commercial (Phywe type) conductometer using a specially designed cell suitable for low conductivity measurement (with a cell constant of $C = 0.875$ cm^{-1}). The temperature was measured using a quartz thermometer (HP 2804A) giving a resolution of 10^{-3} K. The measurement procedure has been designed for obtaining the maximum resolution and for avoiding contamination of the samples. Before any measurement session, the conductometer was calibrated with a certified 10^{-3} mol·L^{-1} KCl solution, and the resolution of the apparatus was 1 % (or 1 nS·cm^{-1} depending on the measured κ value). After calibration, the cell containing the solution was immersed in a thermally stabilized bath with good thermal regulation. The long-time stability of the cell was better than $3 \cdot 10^{-3}$ K. When the temperature of the sample was stabilized, the measurements were made as soon as possible (a few seconds) to reduce any effects that would modify the measured values (such as self heating of the samples, ionization in the electrodes, etc.),[31] and we proceeded to change the temperature for the next measurement. The measurements were reproducible over several hours, showing that the glass electrode was not reacting with the present chemical species.

Refractive Index Measurement. The refractive index of the studied solutions was measured in the temperature interval of (303.315 to 325.476) K by using a thermostatic digital Abbe refractometer at the wavelength of the D line of sodium, 589.3 nm, and under atmospheric pressure. The precision of the measurement is estimated to be $\pm$ 10^{-4}. Temperature was controlled by circulating water into the refractometer through a thermostatically controlled bath with the digital temperature control unit to maintain the desired temperature within $\pm$ 0.01 K. A calibration check was performed by comparing the refractive index of isobutyric acid with the existing data,[32] which were extrapolated at the same temperature and wavelength. The remaining discrepancies amounted to a few 10^{-4} and were on the order of the scatter of the data, as reported by different authors. The sample was injected into the prism assembly by means of an airtight syringe. Refractive index values were measured to an uncertainty of $\pm$ 10^{-4} after the sample mixture was thermostatically equilibrated. To obtain consistent values, we held the temperature constant throughout each set of measurements and repeated every experiment three times under the same conditions.

Theoretical Background and Coexistence Curves. Phase transitions in fluids that are driven by short-range interactions belong to the Ising university class. However the simple power laws involving the universal critical Ising exponents are valid in only the asymptotic region near the critical point.[33,52]

In fact, in binary mixtures, the order parameter M can be chosen to be the difference $M_{u,l} = y_{u,l} - y_c$ of the composition difference of one component between the upper (u) or lower (l) phases of one component and its critical value, y_c. The subscripts u or l refer to the phase above or below, respectively, the meniscus of the earth's gravity field. We write the reduced temperature as $t = T/T_c - 1$. The composition, y, of one component can be written as[35]

$$y_{u,l} = y_c \pm B' t^{\beta}(1 + B_1 t^{\Delta}) + E_y t + G_y t^{1-\alpha} + H_y t^{2\beta} + ... \quad (1)$$

The sign $\pm$ corresponds to the upper (u) or lower (l) phase. In eq 1, the fraction y_c is the critical composition and B' is the first-order correction to the scaling amplitude. F_y, G_y, and H_y are nonuniversal amplitudes. While $\beta = 0.326$, $\Delta = 0.51$ and $\alpha = 0.11$ are the exponents of the 3-dimentional Ising universality class.[35]

In general, the accuracy is not good enough to distinguish between the behaviors t, $t^{1-\alpha} = t^{0.89}$, and $t^{2\beta} = t^{0.65}$; therefore, one can introduce an effective exponent, ω, with amplitude, E_y, whose range will be $\omega = [0.5, 1]$. Equation 1 can be rewritten as

$$y_{u,l} = y_c \pm B' t^{\beta}(1 + B_1 t^{\Delta}) + E_y t^{\omega} \quad (2)$$

In the region not too far from the critical point, power series corrections to the asymptotic power laws may suffice. Then, the prediction for the existence curve involves a power law near critical temperature, T_c, with the exponent β plus nonanalytical corrections;[36−38] far from T_c, the whole enabling the composition difference on one composition between the upper (dioxane-rich) and lower (water-rich) phases involving the reduced temperature, t, can be described by the following equation[34]

$$\Delta y = \left| y_u - y_l \right| = B t^{\beta}(1 + B_1 t^{\Delta} + B_2 t^{2\Delta} + ...) \quad (3)$$

Moreover, the coexistence curve diameter is expected to deviate from the usual linearity governed by the critical exponent $\alpha \approx 0.11$ of the heat capacity, and its equation is expressed as following

$$y_d = \frac{y_u + y_l}{2} = y_c + Dt + D_{1-\alpha} t^{(1-\alpha)}(1 + D_1 t^{\Delta} + ...) + D_{2\beta} t^{2\beta} \quad (4)$$

where y_u and y_l are the conductivity or the refractive index and the (D, $D_{1-\alpha}$, $D_{2\beta}$) amplitudes are temperature independent. The amplitudes B_1 and B_2 of the first Wegner correction are specific for the system.[36]

In eq 4, the second term on the right-hand side is the regular rectilinear dependence, whereas the third and fourth terms represent the nonrectilinear contribution with its correction to simple scaling, as given by a Wegner expansion. The last term takes into account the effect on the diameter of an incorrect choice of the order parameter or, as discussed recently,[53−56] a direct consequence of complete scaling.[22] Equations 3 and 4 can be readily obtained from

$$\left| y - y_c - Dt - D_{1-\alpha} t^{1-\alpha} \right| = \frac{B}{2} t^{\beta}(1 + B_1 t^{\Delta} + B_2 t^{2\Delta} + ...) \quad (5)$$

where $y = y_l$ or y_u (with $y = \kappa$ or n) and $B/2$ is equal to B' in eqs 1 and 2.

The method involves the measurement of the phase separation temperature T_t (the temperature where the meniscus becomes visible) in several samples of different compositions. When the composition is critical, the meniscus appears roughly in the middle of the sample and is displaced either higher or lower if it is not critical. When T_t is in the neighborhood of the phase transition, the main problem of this method, the visual method, is that the meniscus takes place in about 3 h. Gravity effects[39] can also cause experimental artifacts. Clearly, critical opalescence is not a difficulty in this mixture, where the problem is seeing the meniscus, which is possible only if special care is taken.

Table 1. Electrical Conductivity, κ, of Coexisting Phases As a Function of the Temperature

T	κ	κ_l	κ_u	T	κ_l	κ_u
K	mS·cm^{-1}	mS·cm^{-1}	mS·cm^{-1}	K	mS·cm^{-1}	mS·cm^{-1}
304.481	10.11			315.143	26.06	4.406
305.064	10.27			315.302	26.48	4.340
305.652	10.44			315.587	27.19	4.234
306.078	10.58			315.762	27.59	4.206
306.706	10.77			315.917	27.94	4.197
307.144	10.92			316.174	28.53	4.154
307.579	11.07			316.402	29.12	4.032
308.040	11.21			316.616	29.59	4.005
308.777	11.46			316.829	30.10	3.941
309.305	11.65			316.950	30.37	3.923
309.925	11.87			317.080	30.69	3.867
310.380	12.04			317.220	30.93	3.919
310.720	12.18			317.464	31.55	3.798
310.932	12.27			317.896	32.51	3.716
311.061		11.47	8.784	318.318	33.41	3.676
311.108		12.17	8.370	318.742	34.31	3.625
311.178		12.88	8.044	319.254	35.41	3.538
311.220		13.20	7.850	319.550	36.21	3.314
311.290		13.68	7.572	319.843	37.08	3.441
311.368		14.15	7.327	320.215	37.68	3.400
311.522		14.96	6.942	320.383	38.19	3.383
311.741		15.93	6.560	320.790	39.15	3.327
312.030		17.04	6.195	321.274	40.39	3.275
312.319		18.10	5.865	321.830	41.81	3.217
312.548		18.86	5.674	322.182	42.46	3.172
312.763		19.56	5.500	322.457	43.27	3.169
312.973		20.23	5.325	322.848	43.84	3.113
313.235		21.04	5.134	323.380	45.44	3.067
313.407		21.50	5.074	323.770	46.50	3.03
313.607		22.06	4.980	324.149	47.10	2.999
313.685		22.31	4.910	324.439	47.89	2.960
313.799		22.54	4.940	324.856	48.84	2.930
313.915		22.90	4.840	325.326	50.23	2.897
314.106		23.39	4.790	326.031	51.31	2.830
314.235		23.77	4.690	326.864	53.37	2.713
314.513		24.47	4.620	327.592	55.11	2.637
314.702		24.97	4.531	327.918	55.76	2.618
314.971		25.68	4.411			

Results and Discussion

Critical Temperature and Composition. A weakly focused He−Ne laser beam (6328 Å, 5 mW power) was passed through the cell, and the temperature was raised in steps. The critical temperature, T_c^{expt}, was determined by the appearance of a ring of spinodal decomposition in the scattered light after a thermal quench of a few mK. The final states of phase separation have been estimated by the disappearance of the droplets and inhomogeneities, that is, when the fluid becomes transparent. Close to T_c, within a range of about 50 mK, the equilibrium time was very long and could reach 24 h. Experimentally, the lower critical temperature of the system 1,4-dioxane + water + potassium chloride was estimated at $T_c^{expt} = (311.032 \pm 0.015)$ K. As described by Japas and Bianchi,[20] the critical composition used with mole fraction of dioxane on a salt-free basis was $x'_D = n_D/(n_D + n_W) = 0.295 \pm 0.002$, and the molality of the saturated salt at the critical point was $m_s^c = (0.55 \pm 0.05)$ mol·kg^{-1}.

Electrical Conductivity Results. The results of the electrical conductivity, κ, of the coexistence phases of the system 1,4-dioxane + water + potassium chloride are given in Table 1 and depicted in Figure 1. In the second column (Table 1), κ represents the measured conductivity in the one-phase region for critical composition with the mole fraction of dioxane as 0.295 on a salt-free basis and saturated with salt. The other columns correspond to data of the two-phase region. The full set has 61 data points with roughly equal numbers on each side of the critical composition. The data span a range of 17 K above the critical point. Seven points are within the last 0.5 K from the critical temperature, T_c. We observe a slight concavity change when temperature exceeds approximately 10 K to T_c (Figure 1).

Table 2. Refractive Index of Coexisting Phases As a Function of the Temperature

T/K	n	n_l	n_u	T/K	n_l	n_u
303.315	1.3957			314.874	1.3977	1.3882
304.483	1.3955			314.028	1.3976	1.3881
305.658	1.3952			315.134	1.3976	1.3880
306.078	1.3951			315.284	1.3976	1.3879
306.706	1.3950			315.334	1.3975	1.3879
307.144	1.3950			315.474	1.3975	1.3878
307.267	1.3949			315.587	1.3975	1.3878
307.579	1.3949			315.695	1.3975	1.3877
307.790	1.3948			315.819	1.3974	1.3876
308.039	1.3948			315.948	1.3974	1.3875
308.198	1.3948			316.085	1.3973	1.3875
308.289	1.3947			316.267	1.3973	1.3873
308.708	1.3947			316.348	1.3973	1.3873
309.305	1.3946			316.463	1.3972	1.3873
309.395	1.3945			316.710	1.3971	1.3871
309.781	1.3945			316.984	1.3971	1.3870
309.929	1.3944			317.230	1.3970	1.3869
310.193	1.3944			317.407	1.3969	1.3868
310.412	1.3943			317.650	1.3969	1.3866
310.649	1.3943			317.843	1.3968	1.3865
310.720	1.3943			318.021	1.3968	1.3864
310.829	1.3943			318.153	1.3967	1.3864
311.054		1.3961	1.3935	318.268	1.3967	1.3863
311.110		1.3964	1.3932	318.500	1.3966	1.3862
311.165		1.3966	1.3929	318.579	1.3966	1.3862
311.235		1.3968	1.3926	318.799	1.3965	1.3860
311.319		1.3970	1.3923	319.028	1.3964	1.3859
311.409		1.3972	1.3920	319.285	1.3963	1.3858
311.547		1.3974	1.3917	319.463	1.3962	1.3858
311.671		1.3975	1.3914	319.630	1.3962	1.3857
311.842		1.3977	1.3911	319.893	1.3961	1.3855
312.023		1.3978	1.3908	320.095	1.3960	1.3855
312.208		1.3978	1.3905	320.229	1.3960	1.3854
312.392		1.3978	1.3903	320.526	1.3958	1.3853
312.598		1.3979	1.3901	320.739	1.3958	1.3852
312.848		1.3979	1.3898	320.915	1.3957	1.3851
312.990		1.3979	1.3896	321.041	1.3957	1.3850
313.091		1.3979	1.3896	321.281	1.3956	1.3849
313.165		1.3979	1.3895	321.630	1.3955	1.3848
313.240		1.3979	1.3894	321.838	1.3954	1.3847
313.421		1.3979	1.3893	321.936	1.3953	1.3846
313.520		1.9791	1.3892	322.243	1.3952	1.3845
313.601		1.9790	1.3891	322.560	1.3951	1.3844
313.733		1.3978	1.3890	322.935	1.3949	1.3842
313.862		1.3978	1.3889	323.380	1.3947	1.3840
313.973		1.3978	1.3888	323.664	1.3946	1.3839
314.138		1.3978	1.3887	323.815	1.3945	1.3838
314.201		1.3978	1.3887	324.130	1.3943	1.3837
314.260		1.3978	1.3886	324.392	1.3942	1.3836
314.370		1.3978	1.3886	324.641	1.3941	1.3835
314.511		1.3977	1.3885	324.768	1.3940	1.3835
314.614		1.3977	1.3884	325.006	1.3939	1.3834
314.728		1.3977	1.3883	325.249	1.3938	1.3833
314.760		1.3977	1.3883	325.476	1.3937	1.3832

Far from critical temperature, the electrical conductivity difference, $\Delta\kappa$, strongly deviates from the asymptotic behavior (Figure 1). In fact, for many fluid systems, the range of validity of the asymptotic power laws has been found[5−7,20−22,36,37,40−45] to be on the order of only 10^{-3} to 10^{-2} at reduced temperature, t. Also, the Wegner expansion, as a first departure correction,[36,40−42,45] is poorly converging, and one correction to scaling is immediately needed. Then, we must further expand the data range. Moreover, it must be kept in mind that the differences in the molecules size (water and dioxane), dielectric constant, and association or dissociation character play an

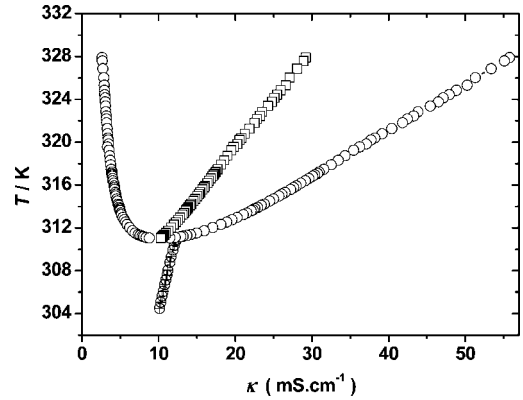

Figure 1. Coexistence curve in the conductivity of lower and upper phases (○), the diameter (□), and the conductivity in the one-phase region (⊕) as a function of the temperature.

important part in these deviations. Going from the water-rich domain to the dioxane-rich domain, the potassium chloride (KCl) passes from a highly soluble strong electrolyte to a scarcely soluble weak electrolyte when association, pairing, and complexing phenomena are accentuated.[1−4,23−29]

To fit the experimental data, eq 3 was used. The amplitude, B, the reduced temperature, t, and the exponent, β, were free. The first-order correction to the scaling amplitude, B_1, was either free or imposed in the fits. The results for the fit of $\Delta\kappa$ at $T <$ 319.800 K (to separate the regular effects) are reported in Table 3. The data analysis was performed using the fitting program OriginPro (7.5). Regarding the amplitudes values of eq 3 completed in the reduced range ($t < 3\cdot10^{-2}$), we can ascertain that the nonclassical Wegner expansion is capable (eq 3) of representing all of our data to within estimated uncertainty.

Within a large domain, correction-to-scaling terms[36] may be added and are usually introduced as eq 3,[34,36] where $\Delta = 0.51$ is supposed to be a universal exponent and the B_1 and B_2 parameters are system-dependent correction-to-scaling amplitudes to be determined by a fitting procedure. The χ^2 goodness-of-fit test was used to optimize the fit and is defined as the following

$$\chi^2 = \frac{1}{N-k}\sum_{i=1}^{i=N}\left(\frac{y_i - y(a_1, ..., a_j, ..., a_k)}{\sigma_i}\right)^2 \qquad (6)$$

where $(N - k)$ is the number of degrees of freedom where N is the number of data points, $y_i = \Delta\gamma$ or Δn, and k is the number of fitted parameters $a_j = (T_c, \beta, B, B_1, \text{and } \Delta)$ in the function $y(a_j)$, and σ_j is the variance of y_i as defined in eq 6.

Note that weighs to the fit variance χ^2 can be used as a criterion for the goodness of the asymptotic model, but one must consider that the χ^2 value is imposed when the number of data points is large. The estimate of the asymptotic value of β obtained by the data regression is highly sensitive to the choice of T_c^{Fit} because the points close to the critical temperature, T_c, that determine the exponent β are the points that are most affected by variation in the T_c. In fit I, when T_c is not fixed to the measured value but is obtained as an adjustable free parameter, the uncertainty in the exponent is increased. In fits III and IV, when $\beta = 0.326$ is fixed, the converging T_c value obtained in fit II has been imposed. We note that the optimum choice of order parameter leads to a fitted T_c^{Fit} value as $T_c =$ (311.013 ± 0.029) K. Note that this value obtained from the fit is very close to the experimental value as $T_c^{exptl} =$ (311.032 ± 0.015) K, and the critical exponent, β, obtained is consistent with the 3D Ising value. Positive B_1 values indicate a monotonic change in the effective exponent with the reduced temperature.

The analysis of the diameter of the coexistence curve was performed by alternatively testing the contributions of the linear term only (fit I), the linear adding singular terms (fit II), and the linear $+2\beta$ terms (fit III). In fact, considered within the renormalization group theory, the mean value of the order parameter y_i should obey the scaling relation expressed by eq 4.[34,41,46] In the present analysis, the nonlinearity of the diameter, as shown in Figure 3, imposes the inclusion of a nonregular contribution to eq 4: either a $1-\alpha$ or 2β term. Therefore, the simplest representations (fits II and III) included one singular term T_c fixed to its experimental value T_c^{exptl}, and the two parameters (D and $D_{1-\alpha}$ for fit II, D and $D_{2\beta}$ for fit II) were adjusted to minimize χ^2. A slightly better performance was obtained for fit III with a (2β) term than for fit II, according to the values of χ^2.

Fits IV and V consider only one free nonregular terms. We ascertain that the $D_{2\beta}$ parameter cannot well represent the whole range as a single nonregular term in eq 4. In fit VI, both nonregular terms were included, and the values of $D_{1-\alpha}$ and $D_{2\beta}$ were adjusted with a considerable improvement in the goodness of fit. Finally, in fit VII, all terms were free. The latter clearly gives the best representations in the extended range studied (far from the consulate point).

The electrical conductivity of the mixture measured in the one-phase region as well as the diameter of the coexistence curve in the two-phase regions changes linearly with temperature. A nonlinear extrapolation of the fit results in the one-phase region and gives $\kappa_c =$ (12.287 ± 0.016) mS·cm^{-1}, whereas the fit of the diameter in the two-phase region gives $\kappa_c =$ (10.233 ± 0.0017) mS·cm^{-1}. The barely detectable difference between the two values, $\delta\kappa_c =$ (2.054 ± 0.018) mS·cm^{-1}, indicates that it is due to the effect of salt.[4−7]

Within the uncertainty of the experiment, no deviations from the law of rectilinear diameter are detectable. In the full range of reduced temperature, the deviations, normalized by the estimated standard deviation, are plotted in Figures 4, 5, 9, and 10 and are defined as $(X_{exptl} - X_{calcd})/\sigma$, where X represents the difference Δy (eq 3) or the diameter y_d (eq 4), and the standard deviation, σ, can be expressed in (eq 7)

$$\sigma = \sqrt{\frac{\sum_{i=1}^{i=N}\left(\frac{n_{i,exptl} - n_{i,calcd}}{n_{i,exptl}}\right)^2}{N-k}} \qquad (7)$$

where N and k are the number of data points and free parameters, respectively.

Figures 4 and 5 show the quality of the fits for electrical conductivity ($\Delta\kappa$ and κ_d) in the two-phase region and over the whole range of explored temperature. With exception, at both ends of the studied reduced temperature range, it is clear that this full-range one-term Wegner fit gives a major improvement and seem to be consistent. Therefore, we have found that the nonclassical Wegner expansion is capable of representing all of our data within estimated uncertainty. Nevertheless, in the t range ends, the noncentered dispersion becomes more nonuniformly distributed, and the deviations are greatly increased and nonhomogeneous. Therefore, this deviation becomes large as the reduced temperature tends to zero or approaches the studied range upper limit ($t < 10^{-3}$ or $t > 5\cdot10^{-2}$). One may notice that the normalized variations for five points near T_c are not compatible with the trend of the points. Note that the variations in Δy and t with absolute temperature T_t very near the consolute point are very sensitive to experimental errors. In fact, it is clear that a small error in upper and lower phases (y_u and y_l,

Table 3. Results for the Fit of the Difference of the Order Parameter in Coexisting Phases According to Equation 3[a]

variable	fit	T_c/K	B	B_1	β	Δ	χ^2
$\Delta\kappa$	I	310.999 ± 0.035	51.784 ± 12.010	6.709 ± 1.686	0.330 ± 0.029	(0.51)	0.053
	II	311.013 ± 0.029	51.507 ± 2.647	6.553 ± 0.348	(0.326)	0.51 ± 0.03	0.320
	III	(311.013)	84.371 ± 6.627	3.533 ± 0.407	0.389 ± 0.010	(0.51)	0.017
	IV	(311.013)	46.076 ± 1.743	6.041 ± 0.139	(0.326)	0.432 ± 0.020	0.0241
Δn	I	311.020 ± 0.011	0.512 ± 0.004	−2.267 ± 0.283	0.331 ± 0.009	0.540 ± 0.062	$3.332\cdot10^{-9}$
	II	311.041 ± 0.009	0.051 ± 0.002	−2.089 ± 0.015	(0.326)	(0.51)	$8.077\cdot10^{-9}$
	III	311.019 ± 0.011	0.054 ± 0.001	−2.147 ± 0.023	0.337 ± 0.004	(0.51)	$3.172\cdot10^{-9}$
	IV	311.029 ± 0.012	0.050 ± 0.008	−2.222 ± 0.146	(0.326)	0.538 ± 0.027	$3.771\cdot10^{-9}$
	V	(311.054)	0.0513 ± 0.0020	−2.049 ± 0.327	(0.326)	0.501 ± 0.064	$8.008\cdot10^{-9}$
	VI	(311.041)	0.051 ± 0.001	−2.079 ± 0.105	(0.326)	0.508 ± 0.020	$8.078\cdot10^{-9}$

[a] T_c, β, and Δ (in parentheses) are fixed in the fitting.

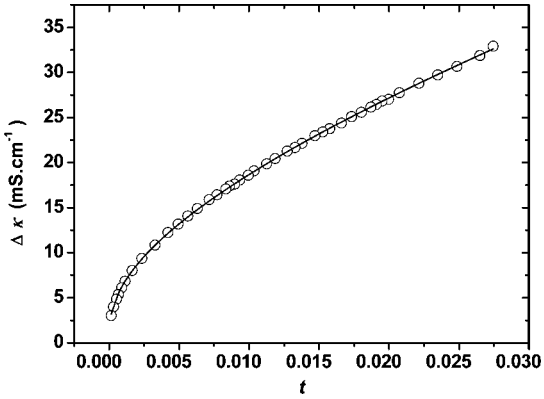

Figure 2. Difference in conductivity of coexistence phases as a function of the reduced temperature, t. Symbols (○) indicate experimental data, whereas the solid line represents the values calculated by fit IV (Table 3).

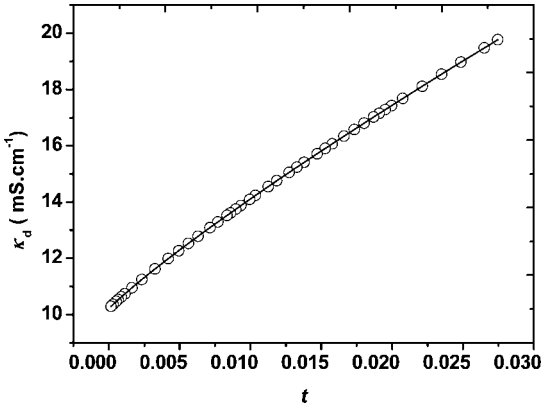

Figure 3. Diameter of the coexistence curve in conductivity as a function of the reduced temperature, t. Symbols (○) indicate experimental data, whereas the solid line represents the values calculated by fit VII (Table 4).

respectively) reflects a very large error in their difference, Δy. We also have the same problem present in the calculation of reduced temperature, t, from the experimental lower critical temperature, T_c^{exptl}, and the phase separation temperature, T_t. Note that the uncertainty of the composition difference, Δy, can exceeds its value for certain data points very near critical temperature, T_c.

Refractive Index Results. The results of the refractive index, n, of coexistence phases of the system 1,4-dioxane + water + potassium chloride are given in Table 2 and depicted in Figure 6.

The results of the fit of Δn are collected in Table 3; the value of $T_c = (311.020 \pm 0.011)$ K obtained from the fit is very close to the experimental value. The critical exponent, β, obtained is consistent with the 3D Ising model. A negative B_1 value indicates a monotonic change in the effective exponent with the reduced temperature.

The results of the diameter fitting are given in Table 4. The analysis of the diameter was performed by alternatively testing the contributions of the linear term only (fit I), the linear term with the addition of singular terms (fit II), and the linear $+2\beta$ terms (fit III).

The refractive index, n, of the mixture measured in the one-phase region as well as the diameter of the coexistence curve in the two-phase region change linearly with temperature. The fit results in the one-phase region give $n_c = 1.39429 \pm 2\cdot10^{-5}$, whereas the fit of the diameter in the two-phase region gives $n_c = 1.39496 \pm 10^{-5}$. The barely detectable difference between the two values ($\delta n_c = 0.00067 \pm 3\cdot10^{-5}$) indicates that the investigation is due to the effect of salt.[4−7]

Within the uncertainty of the experiment, no deviations from the law of rectilinear diameter were detectable.

Effective Exponent. To better characterize the effect of the two corrections to scaling, it is useful to look at the effective β_{eff}, which is defined as follows

$$\beta_{eff} = \frac{\partial \ln(\Delta y)}{\partial \ln t} \tag{8}$$

where Δy defined in eq 3 is the positive difference between order parameters of upper and lower phases and $\Delta y = \Delta\kappa = \kappa_l - \kappa_u$ or $\Delta y = \Delta n = n_u - n_l$. Using eq 3, we can obtain

$$\beta_{eff} = \beta_0 + \frac{B_1\Delta t^{\Delta} + 2B_2\Delta t^{2\Delta}}{1 + B_1 t^{\Delta} + B_2 t^{2\Delta}} \tag{9}$$

Values of the effective exponent, β_{eff}, as a function of reduced temperature, t, were calculated by eq 9. The data analysis was performed using the fitting program OriginPro (7.5) or Kaleidagraph (4.1). In general, the ultimate approach of β_{eff} to its asymptotic value ($\beta_0 = \beta_{Ising} = 0.326$) when $t \rightarrow 0$ is not universal. In particular, when B_1 is positive, the approach is from above (Figure 11), whereas it is from below when B_1 is negative (Figure 12). Note that for our DWKCl system the values of β_{eff} for density values, ρ, investigated in the literature[20] exhibit a shallow minimum followed by a steep increase in the restricted range of reduced temperature to a β_{eff} value near 0.5 at higher distances to consolute point. In this case, mathematical study[46,47] exhibits a small negative B_1 value and a higher positive B_2 parameter in the Wegner corrections when the crossover toward the classical value can be nonmonotonic.

Figures 11 and 12 show the obtained effective exponents, β_{eff}, as a function of the reduced temperature computed from the fit when T_c, β, and Δ are fixed. The value of β_{eff} in the electrical conductivity case (Figure 11) exhibits a steep increase from its asymptotic value of 0.326 to a β_{eff} near the classical value of 0.5 in the restricted range of reduced temperature (t of

Table 4. Results of the Fit of the Coexistence Curve's Diameter of the Order Parameter According to Equation *4*

variable	fit	y_c	D	$D_{1-\alpha}$	$D_{2\beta}$	χ^2
κ_d	I	10.489 ± 0.037	348.335 ± 2.664			0.018
	II	10.165 ± 0.004	−23.521 ± 3.705	251.725 ± 2.505		$7\cdot10^{-5}$
	III	10.088 ± 0.011	241.083 ± 2.575		32.307 ± 0.766	$4\cdot10^{-4}$
	IV	10.185 ± 0.003		235.834 ± 1.593		$1.4\cdot10^{-4}$
	V	9.275 ± 0.010			103.218 ± 1.746	0.088
	VI	10.161 ± 0.005		230.093 ± 1.156	2.542 ± 0.509	$9\cdot10^{-5}$
	VII	10.223 ± 0.002	−211.639 ± 5.193	431.610 ± 4.947	−23.380 ± 0.640	$2.062\cdot10^{-6}$
n_d	I	1.3947 ± 0.0001	−0.13452 ± 0.00048			$3.478\cdot10^{-9}$
	II	1.39485 ± 0.00001	−0.0417 ± 0.0045	−0.0672 ± 0.0032		$0.894\cdot10^{-9}$
	III	1.39489 ± 0.00001	−0.10759 ± 0.00112		−0.01007 ± 0.00 35	$0.308\cdot10^{-9}$
	IV	1.39492 ± 0.00002		−0.09734 ± 0.00020		$1.166\cdot10^{-9}$
	V	1.39562 ± 0.00005			−0.04938 ± 0.00066	$47.95\cdot10^{-9}$
	VI	1.39484 ± 0.00002		−0.10804 ± 0.001	0.0055 ± 0.0007	$0.705\cdot10^{-9}$
	VII	1.39496 ± 0.00001	−0.25341 ± 0.02429	0.14694 ± 0.02446	−0.03143 ± 0.00 350	$0.308\cdot10^{-9}$

about $7\cdot10^{-3}$). In fact, as shown in the literature,[48−50] in ionic systems, the effective exponent, β_{eff}, may display a crossover toward the classical value of 0.5 as T goes away from T_c. This might be explained by the presence of long-range interactions in such ionic mixtures. The positive values of β_{eff} relative to refractive index (Figure 12) exhibit a slight decrease in the asymptotic Ising value of 0.326 to a zero value of β_{eff} in the vicinity of restricted range limit ($t < 4\cdot10^{-2}$). In this domain, when the nonclassical power law is practically absent, the Ising asymptotic behavior is canceled by the two Wegner corrections terms (with B_1 and B_2 amplitudes). Hence, the refractive index difference (Δn) between the upper and lower phases remains constant. Similarly, note that this nonasymptotic vanishing behavior is observed in the literature.[19,50,51] We conclude that this is one reason to emphasize that the fitting experimental data must be done using t values not far from the critical temperature for the eventual determination of asymptotic behavior or Wegner expansion correction.

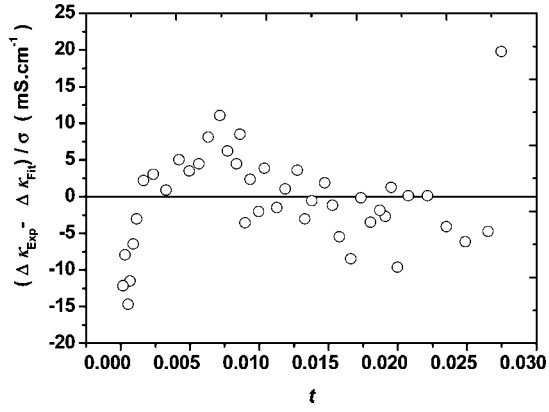

Figure 4. Deviation plot of the difference in conductivity of the coexistence phases as a function of the reduced temperature, t.

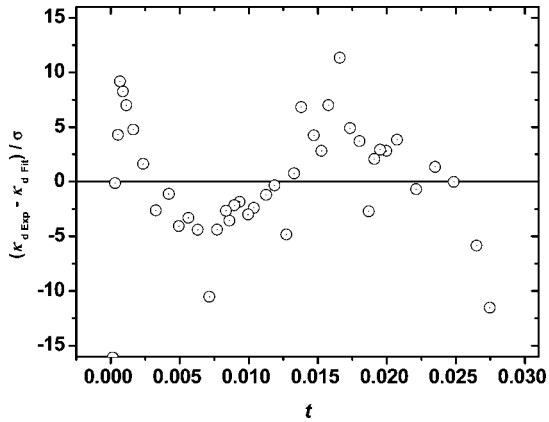

Figure 5. Deviation plot of the coexistence curve's diameter in conductivity as a function of the reduced temperature t.

Conclusions

In this Article, we reported coexistence curves of electrical conductivity and refractive index in the system 1,4-dioxane + water + potassium chloride near and far from its consolute point, which is at 311.032 K and 0.022 mol fraction of KCl with an approximate mole fraction of dioxane of 0.295 on a salt-free basis. Experimental data are reported as a function of reduced temperature. An analysis of our data reveals evidence of nonclassical Ising behavior over almost two decades at reduced

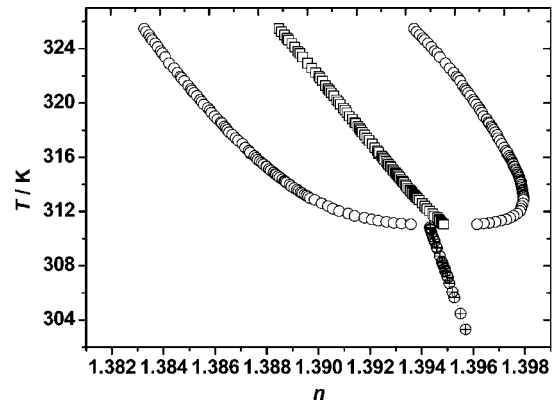

Figure 6. Coexistence curve in the refractive index of the lower and upper phases (○), the diameter (□), and the refractive index in the one-phase region (⊕) as a function of the temperature, t.

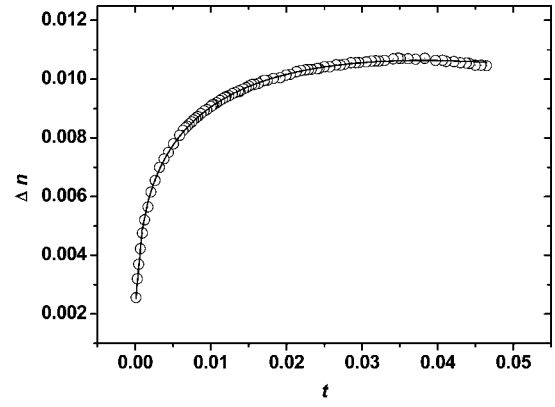

Figure 7. Difference in refractive index of coexistence phases as a function of the reduced temperature, t. Symbols (○) indicate experimental data, whereas the solid line represents the values calculated by fit V (Table 3).

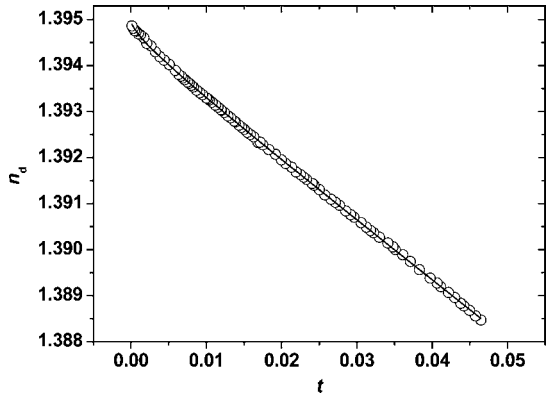

Figure 8. The diameter of the coexistence curve in refractive index n as a function of the reduced temperature, t. Symbols (○) indicate experimental results, whereas the line represents the values calculated by fit IV (Table 4).

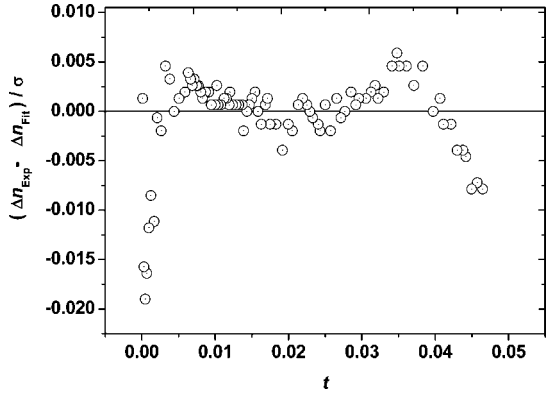

Figure 9. Deviation plot of the difference in refractive index of the coexistence phases as a function of the reduced temperature, t.

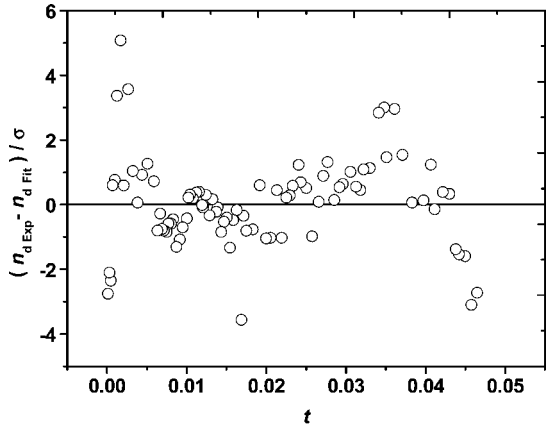

Figure 10. Deviation plot of the coexistence curve's diameter in refractive index n as a function of the reduced temperature, t.

temperature. The range dependence of the asymptotic critical exponent value, the sensitivity of the exponent to error in the critical temperature, and the choice of order parameter are studied. We conclude that not too far from critical temperature, the electrical conductivity constitutes a good order parameter as well as the refractive index to describe the coexistence curve of a critical ternary ionic system as a binary fluid. Far from the consolute point, strong deviation from asymptotic behavior is observed.

The presence of the salt at the saturation in the 1,4-dioaxane and water creates a separation of phase, and the electrolytic system becomes similar to a critical binary mixture as isobutyric acid and water (used in our laboratory). The phenomenon is

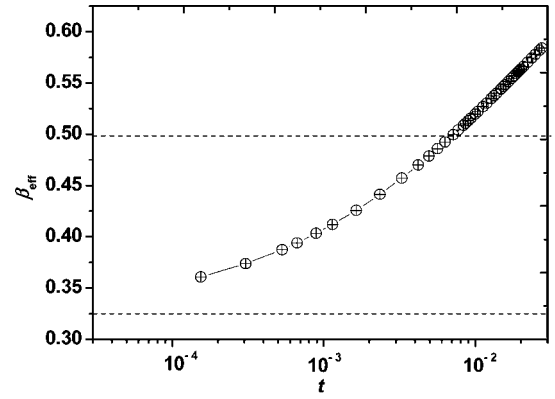

Figure 11. Effective exponent, β_{eff} (eq 9), as a function of the reduced temperature, t, corresponding to the electrical conductivity κ ($B_1 > 0$).

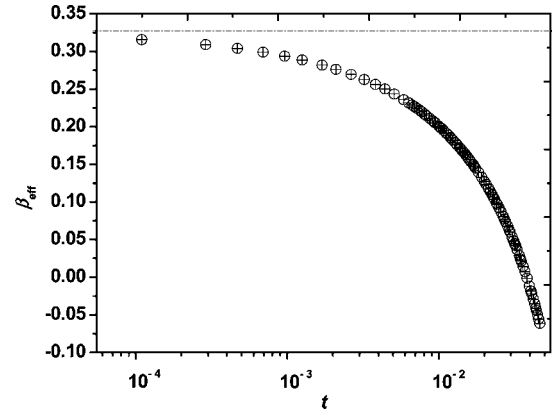

Figure 12. Effective exponent, β_{eff} (eq 9), as a function of the reduced temperature, t, corresponding to the refractive index n ($B_1 < 0$).

characterized by a strong correlation in the critical region. However, the presence of the KCl salt favors the correlation between the molecules of dioxane and water.

Acknowledgment

We thank Professor M. Laura Japas (Unidad de Actividad Química, Comisión Nacional de Energía Atómica, Argentin) for fruitful correspondence and clarifying discussions.

Literature Cited

(1) Bouanz, M. Critical behavior of the self-diffusion coefficient in a binary fluid. *Phys. Rev. A* **1992**, *46*, 4888–4893.
(2) Bouanz, M.; Gharbi, A. Ionic structure in q binary fluid. *J. Phys.: Condens. Matter* **1994**, *6*, 4429–4435.
(3) Bouanz, M. The solvation phenomenon in a binary fluid. *Quim. Anal.* **1996**, *15*, 530–533.
(4) Bouanz, M.; Beysens, D. Effect of ion impurities on a binary mixture of isobutyric acid and water. *J. Chem. Phys. Lett.* **1994**, *231*, 105–110.
(5) Toumi, A.; Bouanz, M. Critical behavior of the binary-fluid isobutyric acid-water with added ion (K^+, Cl^-). *Eur. Phys. J. E* **2000**, *2*, 211–216.
(6) Toumi, A.; Bouanz, M.; Gharbi, A. Coexistence curves of the binary mixture isobutyric acid-water with added ions (K^+, Cl^-). *Chem. Phys. Lett.* **2002**, *362*, 567–573.
(7) Toumi, A.; Bouanz, M.; Gharbi, A. Comportement de la relation de Lorentz-Lorentz dans un mélange binaire critique. *Phys. Chem. News* **2003**, *13*, 126–131.
(8) Kolb, H. A.; Woermann, D. Conductivity fluctuations in butyric acid/water and isobutyric acid/water mixtures. *J. Chem. Phys.* **1984**, *80*, 3781–3784.
(9) Cherif, E.; Bouanz, M. Electrical conductivity along phase diagram of the critical mixture isobutyric acid-water with added (K^+, Cl^-) ions. *Int. J. Mol. Sci.* **2003**, *4*, 326–334.
(10) Cherif, E.; Bouanz, M. Resistivity-viscosity relationship in liquid-liquid critical mixtures with added ions. *Fluid Phase Equilib.* **2007**, *251*, 71–77.

(11) Cherif, E.; Bouanz, M. Coexistence curves of electrical conductivity in critical solution: isobutyric acid-water with added ions. *Phys. Chem. Liq.* **2007**, *44*, 649–661.
(12) Hadded, N.; Bouanz, M. Electrical conductivity of the binary mixture isobutyric acid-water with added (Zn^{2+}, SO_4^{2-}) ions. *Fluid Phase Equilib.* **2008**, *266*, 47–53.
(13) Hadded, N.; Bouanz, M. Excess permittivity and excess conductivity of binary fluid mixture isobutyric acid-water along the coexistence curve Phys. Chem. Liq. **2008**, in press.
(14) Takamuku, T.; Yamaguchi, A.; Matsuo, D.; Tabata, M.; Yamaguchi, T.; Otomo, T.; Adachi, T. NaCl-induced phase separation of 1,4-dioxane-water mixtures studied by large-angle X-ray scattering and small-angle neutron scattering techniques. *J. Phys. Chem. B* **2001**, *105*, 10101–10110.
(15) Bogardus, H. F.; Lynch, C. C. The ternary systems barium chloride-dioxane-water and calcium chloride-dioxane-water. *J. Phys. Chem.* **1943**, *47*, 650–654.
(16) Campbell, A. N.; Kartzmak, E. M.; Maryk, W. B. The systems sodium chlorate-water-dioxane and lithium chlorate-water-dioxane at 25°C. *Can. J. Chem.* **1966**, *44*, 935–937.
(17) Campbell, A. N.; Lam, S. Y. Phase diagrams of sodium chloride and of potassium chloride in water-dioxane. *Can. J. Chem.* **1972**, *50*, 3388–3390.
(18) Bešter, R. M.; Doler, D. Phase equilibria in the (water + 1,4-dioxane + magnesium chloride) system. *Acta. Chim. Slov* **1990**, *46*, 463–470.
(19) Gutkowski, K.; Anisimov, M. A.; Sengers, J. V. Crossover criticality in ionic solutions. *J. Chem. Phys.* **2001**, *114*, 3133–3148.
(20) Bianchi, H. L.; Japas, M. L. Phase equilibria of a near-critical ionic system. Critical exponent of the order parameter. *J. Chem. Phys.* **2001**, *115*, 10472–10478.
(21) Gutkowski, K. I.; Bianchi, H. L.; Japas, M. L. Critical behavior of a ternary ionic system: a controversy. *J. Chem. Phys.* **2003**, *118*, 2808–2814.
(22) Gutkowski, K. I.; Bianchi, H. L.; Japas, M. L. Nonasymptotic critical behavior of a ternary ionic system. *J. Phys. Chem. B* **2007**, *111*, 2554–2564.
(23) Ouerfelli, N.; Ammar, M.; Latrous, H. Ionic self-diffusion coefficients of $^{153}Gd(III)$ in $Gd(NO_3)_3$ solutions in water dioxane mixture at 25 °C. *J. Phys.: Condens. Matter* **1996**, *8*, 8173–8183.
(24) Baker, M. F.; Mohamed, A. A. Ion-Solvent Interaction of Biunivalent Electrolytes in Dioxane-Water Mixtures from Conductivity Data at Different Temperatures. *J. Chin. Chem. Soc.* **1999**, *46*, 899–905.
(25) M'Halla, J.; Besbes, R.; Bouazizi, R.; Boughammoura, S. Ionic condensation of sodium chondroitin sulphate in water-dioxane mixture. *J. Mol. Liq.* **2007**, *130*, 59–69.
(26) M'Halla, J.; Besbes, R.; M'Halla, S. Modélisation des mélanges eau-dioxanne à partir de leur diagramme liquide-vapeur et des mesures de densité et d'enthalpies de mélange. *J. Soc. Chim. Tunis.* **2001**, *4*, 1303–1315.
(27) Bakó, I.; Pálinkás, G.; Dore, J. C.; Fisher, H. E. Structural studies of a water-dioxane mixture by neutron diffraction with hydrogenrdeuterium substitution. *J. Chem. Phys. Lett.* **1999**, *303*, 315–319.
(28) Takamuku, T.; Yamaguchi, A.; Tabata, M.; Nishi, N.; Yoshida, K.; Wakita, H.; Yamaguchi, T. Structure and dynamics of 1,4-dioxane-water binary solutions studies by X-ray diffraction mass spectrometry and NMR relaxation. *J. Mol. Liq.* **1999**, *83*, 163–177.
(29) M'Halla, J.; M'Halla, S. Etude densimétrique etude densimétrique et calorimétrique des systèmes binaire et ternaires (eau/dioxanne/NaB(Ph)$_4$). Effet "clathrate" et solvatation préférentielle de $B(Ph)_4^-$. *J. Chim. Phys.* **1999**, *96*, 1450–1478.
(30) Erdey-Gruz, T. *Transport Phenomena In Aqueous Solutions*; AHPB: London, 1958.
(31) Hamelin, J.; Bose, T. K.; Thoen, J. Dielectric constant and the electrical conductivity near the consolute point of the critical binary liquid mixture nitroethane-3-methylpentane. *Phys. Rev. A* **1990**, *42*, 4735–4742.
(32) Riddick, J. A.; Bunger, W. B; Sakano, T. K. *Organic Solvent, Techiques of Chemistry*, 4th ed.; Wiley-InterScience: New York, 1986; Vol. 1.
(33) Anisimov, M. A.; Kiselev, S. B.; Sengers, J. V.; Tang, S. Crossover approach to global critical phenomena in fluids. *Physica A* **1992**, *188*, 487–525.
(34) Ley-Koo, M.; Green, M. S. Consequences of the renormalization group for the thermodynamics of fluids near the critical point. *Phys. Rev. A* **1981**, *23*, 2650–2659.
(35) *Phase Transitions: Cargése 1980*; Lévy, M., Le Gillou, J.-C., Zinn-Justin, J., Eds.; Plenum: New York, 1982.
(36) Wegner, F. J. Corrections to scaling laws. *Phys. Rev. B* **1972**, *5*, 4529–4536.
(37) Greer, S. C. Coexistence curves at liquid-liquid critical points: Ising exponents and extended scaling. *Phys. Rev. A* **1976**, *14*, 1770–1780.
(38) Beysens, D.; Bourgou, A.; Calmettes, P. Experimental determinations of universal amplitude combinations for binary fluids. I. Statics. *Phys. Rev. A* **1982**, *29*, 3589–3609.
(39) Hohenberg, P. C.; Bartmatz, M. Gravity effects near the gas-liquid critical point. *Phys. Rev. A* **1972**, *46*, 289–313.
(40) Greer, S. C.; Moldover, M. R. Thermodynamic anomalies at critical points of fluids. *Annu. Rev. Phys. Chem.* **1981**, *32*, 233–265.
(41) Kumar, A.; Krishnamurthy, H. R.; Gopal, E. S. R. Equilibrium critical pheneomena in binary liquid mixtures. *Phys. Rep.* **1983**, *98*, 57.
(42) Sengers, J. V.; Levelt Sengers, J. M. H. Thermodynamic behavior of fluids near the critical point. *Annu. Rev. Phys. Chem.* **1986**, *37*, 189–222.
(43) Ley-Koo, M.; Green, M. S. Revised and extended scaling for coexisting densities of SF_6. *Phys. Rev. A* **1977**, *16*, 2483–2487.
(44) Toumi, A.; Bouanz, M. Effect of the (K^+, Cl^-) ions on the order parameters and on the Lorenz-Lorentz relation in the isobutyric acid-water critical mixture. *J. Mol. Liq.* **2005**, *122*, 74–83.
(45) Japas, M. L.; Levelts Sengers, J. M. H. Critical behavior of a conducting ionic solution near its consolute point. *J. Phys. Chem.* **1990**, *94*, 5361–5368.
(46) Bonetti, M.; Oleinikova, A.; Bervillier, C. Coexistence curve of the ionic binary mixture ethylammonium nitrate-*n*-octanol: critical properties. *J. Phys. Chem. B* **1997**, *101*, 2164–2173.
(47) Anisimov, M. A.; Povodyrev, A. A.; Kulikov, V. D.; Sengers, J. V. Nature of crossover between Ising-like and mean-field critical behavior in fluids and fluid mixtures. *Phys. Rev. Lett.* **1995**, *75*, 3146–3149.
(48) Narayanan, T.; Pitzer, K. S. Critical behavior of ionic fluid. *J. Chem. Phys.* **1995**, *102*, 8118.
(49) Singh, R. R.; Pitzer, K. S. Near-critical coexistence curve and critical exponent of an ionic fluid. *Chem. Phys.* **1990**, *92*, 6775–6778.
(50) Povodyrev, A. A.; Anisimov, M. A.; Sengers, J. V. Crossover Flory model for phase separation in polymer solutions. *Physica A* **1999**, *264*, 345–369.
(51) Orkoulas, G.; Panagiotopoulos, A. Z.; Fisher, M. E. Criticality and crossover in accessible regimes. *Phys. Rev. E* **2000**, *61*, 5930–5939.
(52) Wagner, M.; Stanga, O.; Schröer, W. The liquid-liquid coexistence of binary mixtures of the room temperature ionic liquid 1-methyl-3-hexylimidazolium tetrafluoroborate with alcohols. *Phys. Chem. Chem. Phys.* **2004**, *6*, 4421–4431.
(53) Kim, Y. C.; Fisher, M. E.; Orkoulas, G. Asymmetric fluid criticality. I. Scaling with pressure mixing. *Phys. Rev. E* **2003**, *67*, 061506.
(54) Cerdeiriña, C. A.; Anisimov, M. A.; Sengers, J. V. The nature of singular coexistence-curve diameters of liquid-liquid phase equilibria. *Chem. Phys. Lett.* **2006**, *424*, 414–419.
(55) Wang, J.; Anisimov, M. A. Nature of vapor-liquid assymetry in fluid criticality. *Phys. Rev. E* **2007**, *75*, 051107.
(56) Wang, J.; Cerdeiriña, C. A.; Anisimov, M. A.; Sengers, J. V. Principale of isomorphism and complete scaling for binary-fluid criticality. *Phys. Rev. E* **2008**, *77*, 031127.

Received for review July 1, 2008. Accepted November 19, 2008.

JE8005002